ORIGINAL ARTICLE

A proposal for a new analysis of craniofacial morphology by 3-dimensional computed tomography

Sun-Hyung Park,[a] Hyung-Seog Yu,[b] Kee-Deog Kim,[c] Kee-Joon Lee,[d] and Hyoung-Seon Baik[e]
Seoul, South Korea

Introduction: Three-dimensional (3D) analysis is essential for making a precise diagnosis of craniofacial morphology. Two-dimensional (2D) x-ray films are used to understand 3D structures. However, 2D images have several limitations. This article proposes a new type of cephalometric analysis by using 3D computed tomography. **Methods:** Axial images of 30 subjects (16 men; mean age, 19.2 years; 14 women, mean age, 20.5 years) were reconstructed into 3D models by using Vworks 4.0 (Cybermed, Seoul, Korea). The 3D models were measured with Vsurgery (Cybermed). The zygoma, maxilla, mandible, and facial convexity were analyzed. **Results:** The measurements were compared with Korean normal averages, and no statistically significant differences were found. Landmark identification was reproducible. **Conclusions:** Three-dimensional computed tomography can provide information for use in diagnosis and treatment planning. (Am J Orthod Dentofacial Orthop 2006;129:600.e23-600.e34)

From the College of Dentistry, Yonsei University, Seoul, South Korea.
[a]Research fellow, Department of Orthodontics.
[b]Associate professor, Department of Orthodontics.
[c]Associate professor, Department of Oral and Maxillofacial Radiology.
[d]Assistant professor, Department of Orthodontics.
[e]Professor, Department of Orthodontics.
Supported by the Craniofacial Deformity Center of Yonsei University Dental Hospital.
Reprint requests to: Hyoung-Seon Baik, 134 Shinchondong, Seodaemungu, Department of Orthodontics, College of Dentistry, Yonsei University, Seoul, South Korea 120-752; e-mail, baik@yumc.yonsei.ac.kr.
Submitted, August 2005; revised and accepted, November 2005.

Three-dimensional (3D) analysis is essential for precisely assessing craniofacial morphology. Two-dimensional (2D) x-ray films have been used to depict 3D structures, but they have several limitations. In lateral cephalometry, it is difficult to determine the difference between the left and right sides for superimposing images, and the sides have

0889-5406/$32.00

doi:10.1016/j.ajodo.2005.11.032

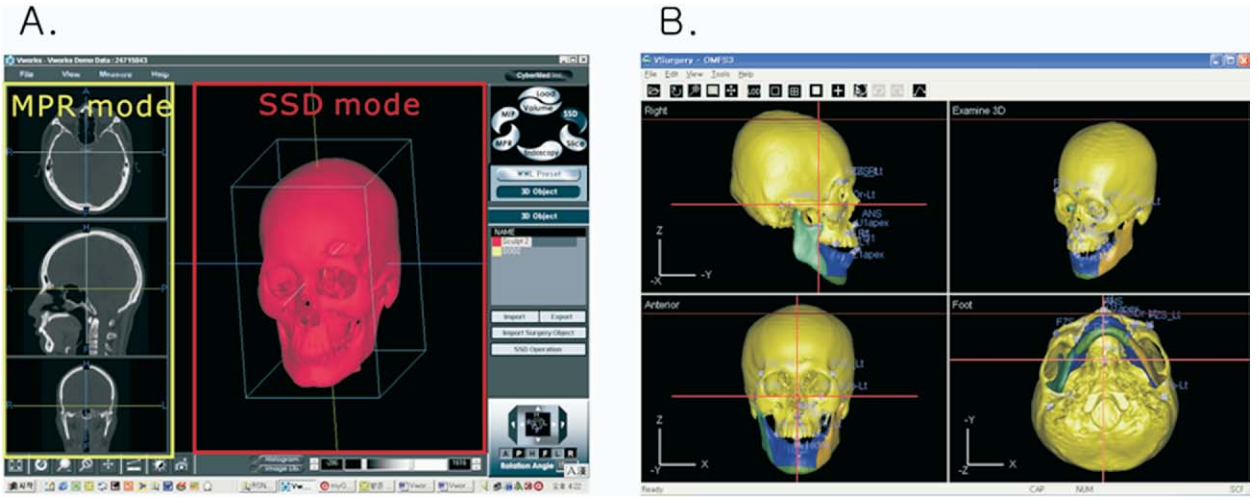

Fig 1. A, 3D model made by Vworks. Multiple planar reformat mode shows axial, coronal, and sagittal views of landmarks. Shaded surface display mode creates 3D model that can be rotated and viewed from any angle. **B,** 3D model made by Vworks imported to Vsurgery.

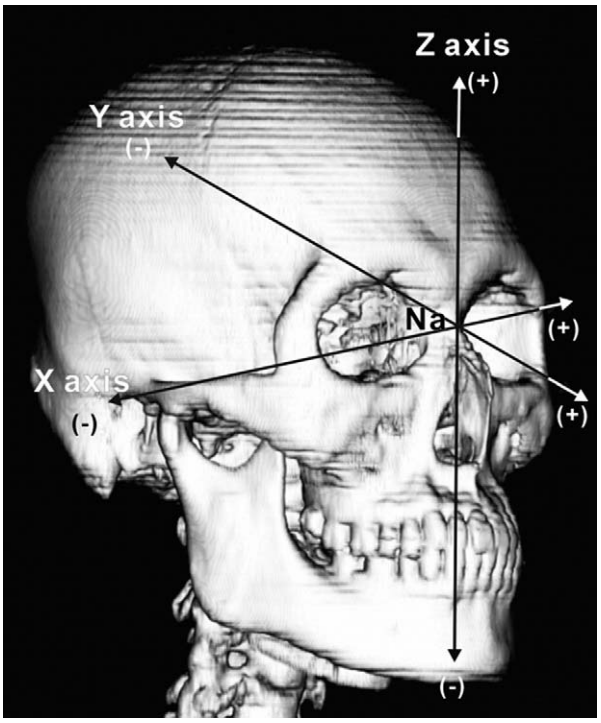

Fig 2. X-, y-, and z-coordinates in this study.

different enlargement ratios. In addition, deformities in the midfacial area cannot always be detected. In posteroanterior and basilar cephalometry, the images can be distorted by the patient's head position during the imaging process. Moreover, reading the films can be complicated because of the superimposition of cranial structures.

Many techniques have been developed to compensate for the drawbacks of 2D measurements. These include the orietator,[1] the coplanar stereometric system,[2] the multiplane cephalometric anaylsis,[3] the basilar multiplane cephalometric analysis,[4] and the biplanar cephalometric stereoradiography.[5]

Three-dimensional computed tomography (CT) is widely used in dentistry for many reasons: (1) actual measurements can be obtained,[6] (2) a spatial image of the craniofacial structures can be produced, (3) the 3D image can be rotated easily by changing the rotational axis, (4) the inner structures can be observed by removing the outer surfaces,[7] and (5) various organs can be observed independently by changing the density of the organs. A 3D CT image can also show asymmetry of the midface and the cranial base; this is difficult to detect with ordinary 2D x-ray film.[8,9] Despite the usefulness and versatility of CT, the high cost of a 3D CT reconstruction and the radiation exposure required are disadvantages. Therefore, 3D CT can be used in conjunction with routine 2D CT.[10,11] Lee[12] and Hwang et al[13] reported that a combination of lateral, posteroanterior, and basilar cephalometry provided the same result as 3D CT. However, to obtain this result, accurate positioning of the patient when taking the lateral and posteroanterior cephalograms is essential.

Many studies have evaluated the clinical applicability of 3D CT. Cavalcanti and Vannier[6] reported that the

Table I. Landmarks used in study

Landmark	*Definition*
P (prechiasmatic groove)	Vertical and transverse midpoint of prechiasmatic groove
Na (nasion)	Most posterior point on curvature between frontal bone and nasal bone in midsagittal plane
Or (orbitale)	Lowest point on infraorbital margin of each orbit
ANS (anterior nasal spine)	Most anterior point of nasal floor
A (subspinale)	Most posterior point on curve between ANS and prosthion (Pr)
B (supramentale)	Most posterior point of bony curvature of mandible below infradentale and above Pog
Pog (Pogonion)	Most anterior midpoint of symphysis of mandible
Me (menton)	Most inferior point on symphysis of mandible
PNS (posterior nasal spine)	Most posterior and middle point on contour of bony palate
Po (porion, anatomical)	Highest midpoint on roof of external auditory meatus
CP (condylion posterioris)	Most upper and posterior aspect of condyle
Go1 (gonion1)	Most posterior point of posterior border of ramus
Go2 (gonion2)	Midpoint of posterior border of mandibular angle
Go3 (gonion3)	Most inferior point of posterior border of ramus
Mx (maxillare)	Zygomaticoalveolar crest, points show maximum concavity on contour of maxilla around molars and lower contour of maxillozygomatic process
ZP (zygion point)	Most lateral point where zygomatic arch is widest
Bc (buccale)	Point on external surface of each zygomatic arch where arch turns medially and directly starts on backward sweep
R (anterior ramus point)	Deepest point at anterior border of ramus
Pr (prosthion)	Point of maxillary alveolar process between left and right maxillary incisors

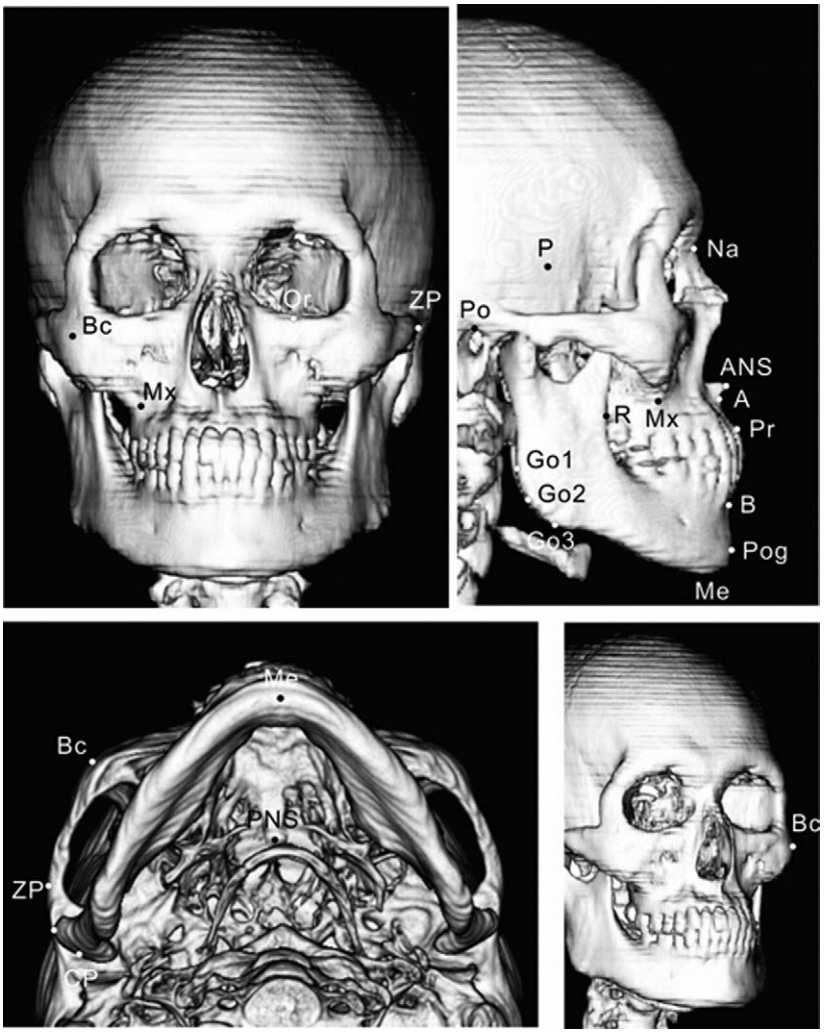

Fig 3. Nineteen landmarks used in study. See Table I for definitions.

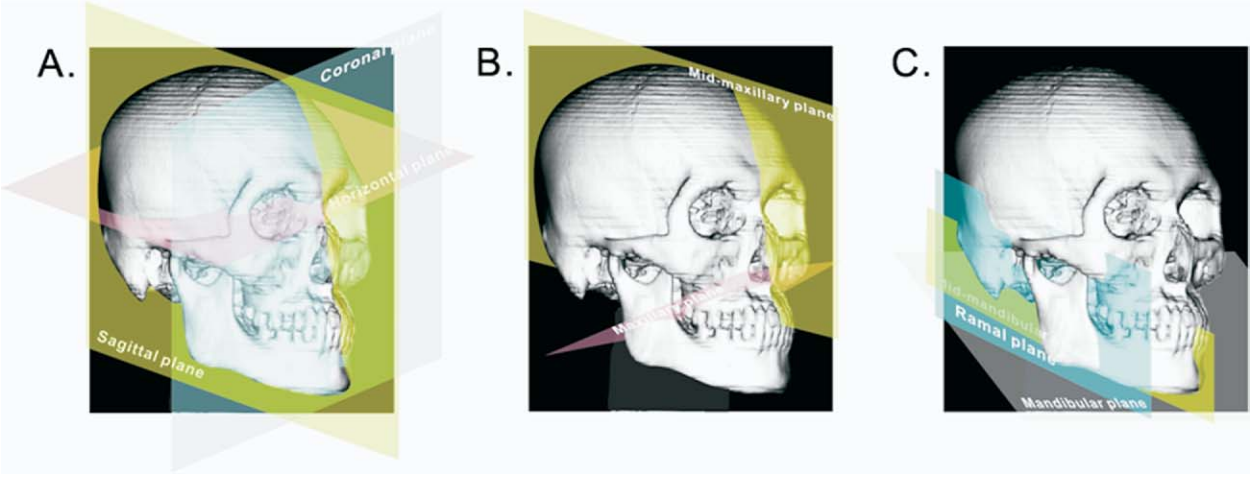

Fig 4. Nine reference planes used in this study.

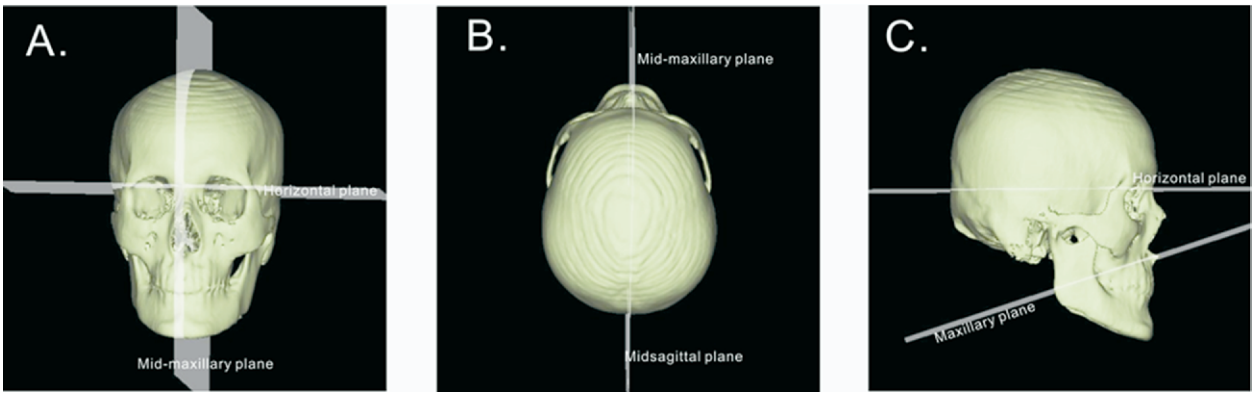

Fig 5. Maxillary measurements: **A,** canting; **B,** rotation; **C,** divergence.

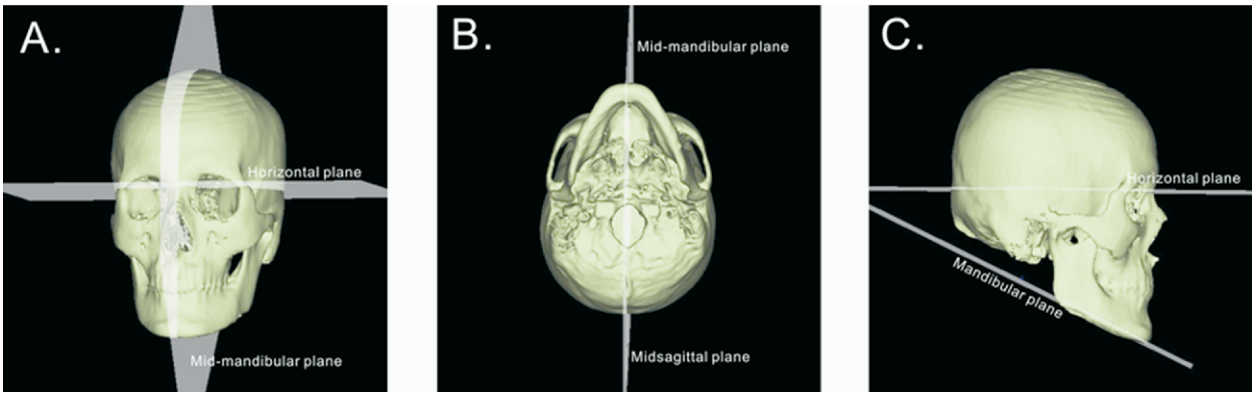

Fig 6. Mandibular measurements: **A,** canting; **B,** rotation; **C,** divergence.

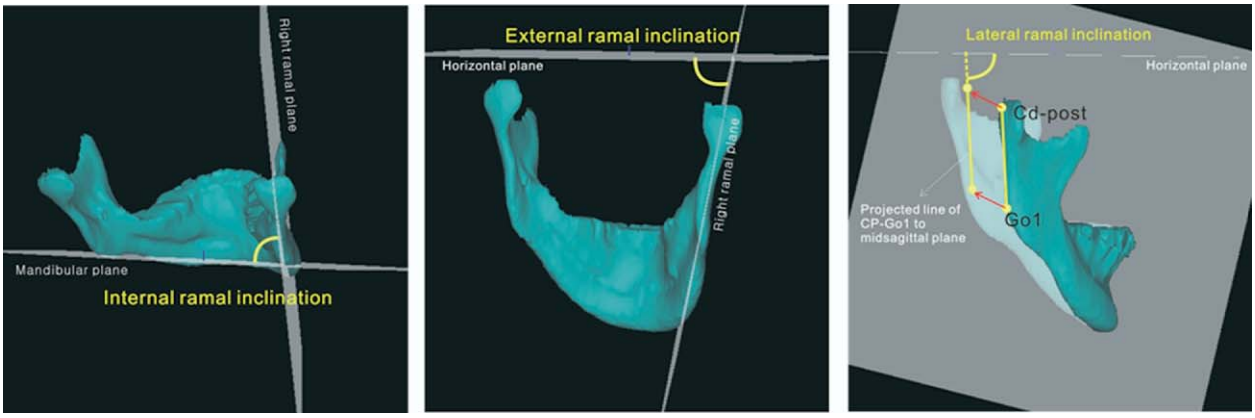

Fig 7. Internal ramal inclination, external ramal inclination, and lateral ramal inclination.

difference between direct measurements of the cranial bone and indirect measurements using a 3D image was within 2 mm. Chang[14] and Kim[15] proposed the use of highly reproducible landmarks in 3D CT. However, there has been no organized analysis of craniofacial deformities with 3D CT. This article proposes a new method for cephalometric analysis with 3D CT and shows the method used for a patient with facial asymmetry.

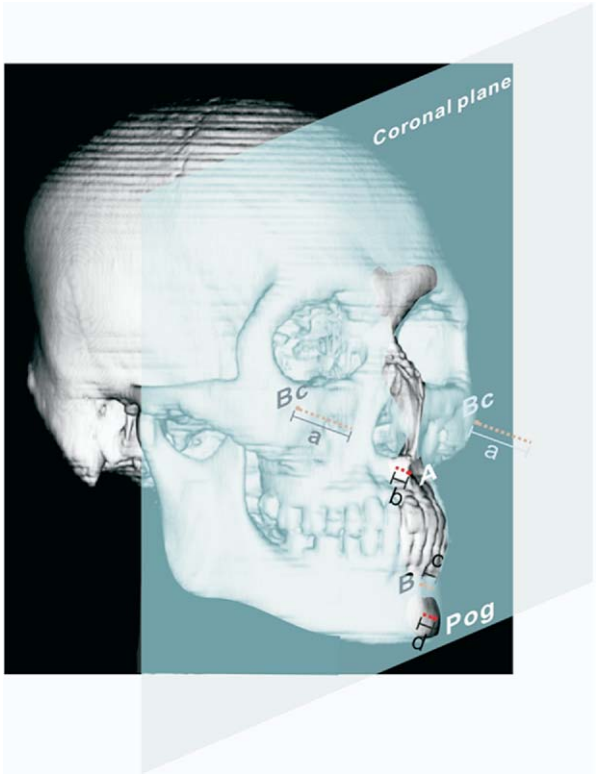

Fig 8. Facial convexity: *a,* distance from coronal plane to Bc; *b,* distance from coronal plane to A; *c,* distance from coronal plane to B; *d,* distance from coronal plane to Pog. Facial convexity is calculated by 1: b/a : c/a : d/a.

MATERIAL AND METHODS

Clinical examinations were carried out on 30 students from Yonsei University, and lateral cephalometric records and study models were collected. Each subject had normal occlusion and a balanced face. Students who had previously received orthodontic treatment were excluded. The sample consisted of 16 men (mean age, 19.2 years) and 14 women (mean age, 20.5 years). The CT images were made with a CT Hispeed Advantage (GE Medical System, Milwaukee, Wis) with a high-resolution bone algorithm, 512 × 512 matrix, 120 KV, and 200 mA. The thickness of the axial images was 3 mm, the table speed was 6 mm per second, and the 3D image was reconstructed with a 2 mm slice thickness. The subjects were positioned with the Frankfort horizontal (FH) line perpendicular to the floor and the facial midline coinciding with the long axis of the CT machine. The image covered the area from the vertex to the inferior border of the mandibular body.

The axial images were reconstructed into a 3D model by using Vworks 4.0 (Cybermed, Seoul, Korea) (Fig 1, *A*). The Vworks 4.0 and Vsurgery (Cybermed) programs were used to measure the 3D models (Fig 1, *B*). Landmarks were first designated on the 3D surface model, and their positions were verified in multiple planar reformat mode. A positive coordinate value indicates the front, superior, and left side of the patient, and a negative value indicates the opposite (Fig 2). Landmarks are defined in Table I and illustrated in Figure 3.

To assess reproducibility of the landmarks, a subject was chosen at random, and 19 landmarks were identified 5 times in 1 session by an operator (S.H.P.) 2 weeks after the first session. A paired *t* test between the 2 sessions was carried out by using SAS version 8.2 (SAS, Cary, NC).

The horizontal reference plane was established parallel to the FH plane, which was constructed on both sides of Po and left of Or, passing through Na (see Table I for definitions). The midsagittal plane was drawn perpendicular to the horizontal plane passing through Na and P. The coronal plane was at right angles to the horizontal and midsagittal plane passing through Na. The maxillary plane was made by the right and left Mx and ANS. The midmaxillary plane was perpendicular to the maxillary plane passing through ANS and PNS. The mandibular plane was constructed by Me and both sides of Go2. The midmandibular plane was perpendicular to the mandibular plane passing through Me and the midpoint of right and left Go2($Go2_M$). R, Go1 and CP formed the ramal plane on both sides (Fig 4).

Vsurgery was used to automatically calculate the linear and angular measurements, with the exception of the internal and external ramal inclinations, which were calculated with Vworks. This software has a 3D tool that can measure an angle between 2 planes.

The following measurements were determined for the zygoma: (1) facial index, ([Na-Me distance]/[distance between right and left ZP]) × 100%; (2) midface angle, Pr-Mx-Bc; and (3) Bc point, the 3D coordinates of both Bc points.

In the maxilla, the following measurements were made (Fig 5): (1) canting, angle between the horizontal and midmaxillary planes (a positive value indicated a counterclockwise rotation; (2) rotation, angle between the midsagittal and midmaxillary planes (a positive value indicated that the midmaxillary plane is left of the midsagittal plane); (3) divergence, angle between the horizontal and maxillary planes (a positive value indicates that ANS is superior to PNS); (4) A-point, 3D coordinates of A; and (5) PNS point, 3D coordinates of PNS.

The following mandibular measurements were made (Fig 6): (1) canting, angle between the horizontal and midmandibular planes; (2) rotation, angle between the midsagittal and midmandibular planes (a positive value indicates that the midmandibular plane is left of

Table II. Cephalometric values of subjects in study and normal values

	M (exp)		*M (normal)*		*F (exp)*		*F (normal)*	
	Mean	*SD*	*Mean*	*SD*	*Mean*	*SD*	*Mean*	*SD*
SNA angle (°)	80.8	3.4	82.5	3.2	82.8	2.9	81.6	3.2
SNB angle (°)	78.5	4.2	80.4	3.1	79.5	2.9	79.2	3.0
ANB angle (°)	2.3	1.7	2.1	1.8	3.3	0.8	2.5	1.8
Sum (°)	391.6	7.3	390.3	5.5	396.0	4.9	393.2	5.2
Mn plane angle (°)	31.6	7.3	30.3	5.5	36.0	4.9	33.4	5.1
Upper lip (mm)	−2.0	2.3	−0.7	2.2	−0.7	1.8	−0.9	2.2
Lower lip (mm)	−0.1	2.4	0.5	2.3	1.6	1.7	0.6	2.3
U1 to SN (°)	106.3	6.4	108.7	5.7	104.5	5.0	106.9	6.0
IMPA (°)	96.0	6.2	96.6	6.6	93.0	4.8	95.9	6.4

M, Male; *F,* female; *exp,* experimental.

Table III. Standard deviations (mm) of 19 landmarks and intraexaminer reliability test between 2 sessions

	Normal				*Patient*			
Landmarks	*x*	*y*	*z*	*Sig*	*x*	*y*	*z*	*Sig*
Po								
R	0.57	0.48	0.89	NS	0.36	0.19	0.00	NS
L	0.65	0.53	0.89	NS	0.86	0.24	0.00	NS
Or								
R	0.53	0.38	0.00	NS	0.76	0.89	0.00	NS
L	0.52	0.49	0.00	NS	0.58	0.93	0.89	NS
Na	0.24	0.30	0.89	NS	0.19	0.19	1.10	NS
P	0.36	0.36	0.00	NS	0.38	0.19	0.00	NS
ANS	0.36	0.19	0.00	NS	0.00	0.30	0.00	NS
A	0.00	0.47	0.00	NS	0.19	0.19	1.10	NS
Pr	0.00	0.19	0.89	NS	0.19	0.36	1.41	NS
PNS	0.36	0.47	0.00	NS	0.36	0.38	0.00	NS
Mx								
R	0.53	0.59	0.89	NS	0.59	0.56	1.10	NS
L	0.47	0.51	0.89	NS	0.42	0.36	0.89	NS
Bc								
R	0.53	0.72	1.10	NS	0.36	0.72	1.10	NS
L	0.48	0.61	1.10	NS	0.56	0.33	1.10	NS
ZP								
R	0.56	0.52	0.89	NS	0.00	0.65	0.00	NS
L	0.36	0.93	1.41	NS	0.38	0.64	0.89	NS
B	0.00	0.01	0.00	NS	0.56	0.58	1.10	NS
Pog	0.23	0.23	1.10	NS	0.77	0.19	0.00	NS
Me	0.30	0.43	0.00	NS	0.24	0.36	0.89	NS
Go1								
R	0.24	0.83	1.41	NS	0.38	0.23	1.10	NS
L	0.58	0.19	0.89	NS	0.47	0.36	1.10	NS
Go2								
R	0.43	0.77	1.67	NS	0.24	0.72	1.10	NS
L	0.56	0.47	0.89	NS	0.30	0.24	1.10	NS
Go3								
R	0.49	0.90	0.89	NS	0.65	0.80	0.89	NS
L	0.51	0.67	1.10	NS	0.71	0.65	0.00	NS
CP								
R	0.36	0.36	0.89	NS	0.43	0.38	1.10	NS
L	0.23	0.24	1.00	NS	0.23	0.03	0.89	NS
R								
R	0.00	0.58	1.10	NS	0.00	0.30	1.10	NS
L	0.36	0.19	1.10	NS	0.85	0.48	1.10	NS

NS, Not significant ($P > .01$); *R,* right; *L,* left.

Table IV. Means and standard deviations of subjects' measurements

	Male (n = 16)		*Female (n = 14)*	
	Mean	*SD*	*Mean*	*SD*
Zygoma				
Facial index	87.1	4.7	88.8	5.9
Midface angle				
R	125.9	8.8	129.0	8.5
L	126.0	7.7	130.6	6.8
diff	−0.1	2.9	0.1	2.7
Maxilla				
Canting (°)	0.5	1.3	0.4	1.2
Rotation (°)	0.1	1.6	−0.6	0.9
Divergence (°)	−6.7	4.8	−21.3	3.6
Mandible				
Canting (°)	0.0	1.2	0.3	1.5
Rotation (°)	−1.1	1.8	−.8	1.4
Divergence (°)*	27.4	4.2	30.9	5.8
Mandibular measurements				
Body length (mm)				
R	94.7	5.2	88.9	3.9
L	96.8	5.9	91.5	2.8
diff	−1.3	2.4	−2.8	2.6
Gonial angle				
R	118.9	4.4	125.0	4.3
L	118.6	5.4	123.6	5.3
diff	0.6	2.0	1.4	1.9
Ramus height (mm)				
R*	60.7	6.4	51.5	2.7
L	60.0	7.2	50.5	4.2
diff	1.0	4.6	1.9	4.9
Internal ramal inclination (°)				
R	91.9	4.3	90.3	5.3
L	91.9	5.1	91.4	4.6
diff	0.0	1.4	−1.1	1.4
External ramal inclination (°)				
R	80.6	3.3	82.2	4.3
L	81.0	2.6	81.4	3.6
diff	−0.4	1.8	0.8	2.0
Lateral ramal inclination (°)				
R	86.0	2.5	83.4	3.2
L	85.7	2.5	85.0	3.6
diff	0.2	1.8	−1.4	1.6
Chin prominence (mm)				
Abs	4.6	0.8	4.0	0.6
Rel.	4.7	0.8	4.4	0.6
Mn-face width	1.0	0.1	1.0	0.0
Landmarks 3D coordinates				
Bc (mm)				
R				
x*	−53.6	3.2	−49.5	2.7
y	−17.3	3.8	−14.8	2.2
z	−34.2	4.2	−31.1	4.8
L				
x*	53.4	3.1	49.3	1.5
y	−16.5	4.5	−14.7	2.4
z	−35.4	5.4	−31.4	3.9
Mx (mm)				
R				
x*	−32.4	1.3	−29.4	1.4
y	−20.1	3.2	−17.3	1.4
z	−61.8	3.4	−59.1	4.2

Table IV. Continued

	Male (n = 16)		*Female (n = 14)*	
	Mean	*SD*	*Mean*	*SD*
L				
x	31.1	2.1	28.7	1.9
y	−20.7	3.7	−17.5	0.8
z	−62.5	3.7	−58.5	4.0
A (mm)				
x	−0.9	0.8	−0.7	0.8
y	−0.6	3.3	0.3	2.1
z	−60.3	3.5	−56.3	3.3
PNS (mm)				
x	−0.9	1.1	−0.2	1.1
y	−48.0	4.9	−43.4	3.0
z	−55.0	4.1	−51.4	4.1
B (mm)				
x	−0.8	1.4	0.4	1.8
y	−5.6	4.4	−3.6	4.4
z	−101.0	3.2	−97.7	5.4
Pog (mm)				
x	−1.1	1.6	0.4	1.8
y*	−6.1	5.3	−3.8	4.6
z	−115.6	3.2	−110.7	4.2
Me (mm)				
x	−1.2	1.7	0.5	1.8
y*	−10.5	6.2	−10.3	4.3
z	−124.7	3.0	118.5	4.7
Facial convexity				
Bc:A:B:Pog				
R	1:−0.0:0.1:0.1	−:0.2:0.4:0.4	1: −0.1:0.2:0.2	−:0.1:0.3:0.3
L	1:−0.0:0.1:0.1	−:0.2:0.4:0.4	1: −0.1:0.2:0.2	−:0.1:0.3:0.3

*Statistically significant differences between men and females ($P < .01$).
R, Right; *L,* left; *diff,* difference.

the midsagittal plane); (3) divergence, angle between the horizontal and mandibular planes (a positive value indicates that Me is inferior to $Go2_M$); (4) body length, (Me-Go3 distance) + (Go3-Go2 distance); (5) ramal height, (CP-Go1 distance) + (Go1-Go2 distance); (6) gonial angle, CP-Go2-Me; (7) chin prominence, "absolute chin prominence" was the perpendicular distance from the Pog to B-Me line; "relative chin prominence" was the absolute chin prominence divided by mandibular body length (average of right and left lengths); (8) internal ramal inclination, angle formed by the ramal and mandibular planes, representing the angle between the ramus and the body of the mandible (Fig 7); (9) external ramal inclination, angle formed by the horizontal plane and right and left ramal plane, indicating the ramal inclination toward the cranial base (Fig 7); (10) lateral ramal inclination, assessed by drawing a perpendicular line from the CP and Go1 onto the midsagittal plane; the lateral ramal inclination was the angle made by the y-axis, the left and right Go1-CP line projected to the midsagittal plane. The right and left angles were measured (Fig 7), showing the anteroposterior inclination of the ramus toward the horizontal plane; (11) B-point, 3D coordinates of B; (12) Pog point, 3D coordinates of Pog; (13) Me point, 3D coordinates of Me; and (14) mandibular-facial width (Na-Me distance)/(distance between $Go2_R$ and $Go2_L$).

The facial convexity measurment indicated the protrusive state of Bc, A, B, and Pog to the coronal plane, and was expressed as a ratio of the z-coordinate of the 4 points. The z-coordinates of A, B, and Pog were divided by that of the right side Bc (Fig 8).

Seven bilateral measurements were made: mandibular body length; gonial angle; ramal height; internal, external, and lateral inclination; and midface angle. Right and left side measurements were compared, and the following ratio was used to express the difference: differential ratio = ([right side value − left side value]/[average of right and left values]) × 100%.

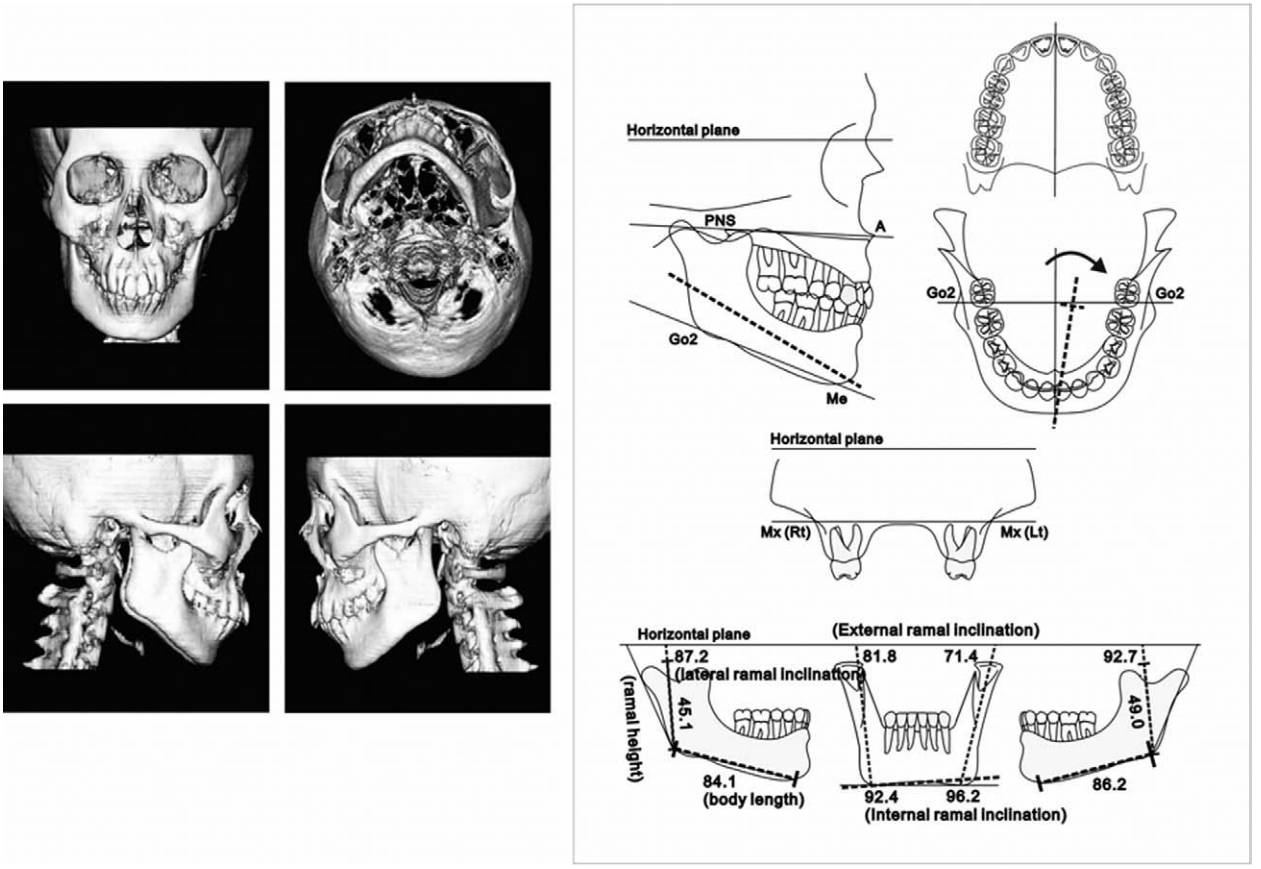

Fig 9. A, 3D CT of patient with asymmetry; **B,** 3D chart.

RESULTS

The cephalometric measurements of the subjects were compared with Korean normal averages (*t* test, $P < .01$, Table II), and no statistically significant differences were found. All landmarks were reproducible, and there was no significant intraexaminer error between the 2 sessions (Table III, $P > .01$). Eight measurements differed between the men and the women (Wilcoxon 2-sample test, $P < .01$), and these are marked with asterisks in Table IV.

A man, age 21.5 years, visiting the Craniofacial Deformity Center of Yonsei University Dental Hospital for management of facial asymmetry, was evaluated (Fig 9, Table V). He had a retrusive mandible with maxillary and mandibular rotation to the left side. Rotation was observed in the posterior area but not in the anterior area (x-coordinate of Me was on midline). This rotation might have been due to a longer body length and ramal height on the right side as well as a different condylar direction (there was a large difference in lateral ramal inclination). In addition, chin prominence was smaller than normal.

DISCUSSION

Many studies have combined lateral, anteroposterior, and basilar cephalometry, which is familiar to orthodontists, to determine the actual 3D position of landmarks. However, 2D images have distinct limitations, including image distortion and overlapping of the head structures, and they are influenced by the patient's head position. Moreover, 2D images provide inconsistent information in some types of deformities.[12,16] Therefore, many clinicians use 3D CT to overcome these limitations and better understand the spatial structures.

The 3D analysis proposed here examines the zygoma, maxilla, mandible, and facial convexity. The facial index is the ratio of zygomatic width tovertical facial height. In anthropometric aspects, the average facial index ranges from 85% to 89.99%, and the face is called "mesoprosopy."[17] Our normal subjects were

Table V. 3D analysis of 1 patient

	Male (Mean ± SD)	*Patient*	
		Measurement	*Deviation*
Zygoma			
Facial index	87.1 ± 4.7	86.9	—
Midface angle			
R	125.9 ± 8.9	128.6	—
L	126.0 ± 7.7	123.9	—
diff	−0.1 ± 2.9	3.8	↑
Maxilla			
Canting (°)	0.5 ± 1.3	1.0	—
Rotation (°)	0.1 ± 1.6	−1.7	↓
Divergence (°)	−16.7 ± 4.8	−18.3	—
Mandible			
Canting (°)	0.0 ± 1.2	−1.7	↓
Rotation (°)	−1.1 ± 1.8	−2.0	—
Divergence (°)	27.4 ± 4.2	32.8	↑ ↑
Mandibular measurements			
Body length (mm)			
R	94.7 ± 5.3	84.1	↓ ↓
L	96.8 ± 5.9	86.2	↓ ↓
diff	−1.3 ± 2.4	−2.5	—
Gonial angle (°)			
R	118.9 ± 4.4	118.1	—
L	118.6 ± 5.4	119.9	—
diff	0.6 ± 2.0	−1.5	↓
Ramus height (mm)			
R	60.7 ± 6.4	45.1	↓ ↓
L	60.6 ± 7.2	49.0	↓
diff	1.0 ± 4.6	−8.4	↓ ↓
Internal ramal inclination (°)			
R	91.9 ± 4.3	93.1	—
L	91.9 ± 5.1	96.9	—
diff	0.0 ± 1.4	−4.0	↓ ↓
External ramal inclination (°)			
R	80.6 ± 3.3	84.3	↑
L	81.0 ± 2.6	72.4	↓ ↓ ↓
diff	−0.4 ± 1.8	15.2	↑ ↑ ↑ ↑ ↑ ↑ ↑ ↑
Lateral ramal inclination (°)			
R	86.0 ± 3.3	81.8	↑
L	85.7 ± 2.5	71.4	↑
diff	0.2 ± 1.8	10.4	—
Chin prominence (mm)			
Abs	4.6 ± 0.8	2.3	↓ ↓
Rel	4.7 ± 0.8	2.7	↓ ↓
Mn-face width	0.9 ± 0.1	0.9	—
Landmarks coordinates			
Bc (mm)			
R			
x	−53.6 ± 3.2	−45.9	↑ ↑
y	−17.3 ± 3.8	−11.6	↑
z	−34.2 ± 4.2	−24.9	↑ ↑
L			
x	53.4 ± 3.1	48.2	↓
y	−16.5 ± 4.5	−12.7	—
z	−35.4 ± 5.4	−25.1	↑
Mx (mm)			
R			
x	−32.4 ± 1.3	−25.8	↑ ↑ ↑ ↑ ↑
y	−20.1 ± 3.2	−13.6	↑ ↑
z	−61.8 ± 3.4	−56.2	↑

Table V. Continued

	Male (Mean ± SD)	Patient	
		Measurement	Deviation
L			
x	31.1 ± 2.1	27.9	↓
y	−20.7 ± 3.7	−17.4	—
z	−62.5 ± .7	−55.3	↑ ↑
A (mm)			
x	−0.9 ± 0.8	0.3	↑
y	0.6 ± 3.3	1.5	—
z	−60.3 ± 3.5	−53.0	↑ ↑
PNS (mm)			
x	−0.9 ± 1.1	0.7	↑
y	−48.0 ± 4.9	−42.8	↑
z	−55.0 ± 4.1	−46.7	↑ ↑
B (mm)			
x	−0.8 ± 1.4	−0.1	—
y	−5.6 ± 4.4	−11.3	↓
z	−101.0 ± 3.2	−97.0	↑
Pog (mm)			
x	−1.1 ± 1.6	−0.1	—
y	−6.6 ± 5.3	−11.2	—
z	−115.6 ± 3.2	−102.6	↑
Me (mm)			
x	−1.2 ± 1.7	−0.2	—
y	−10.5 ± 6.2	−16.2	—
z	−124.7 ± 3.0	−108.8	↑ ↑ ↑ ↑ ↑
Facial convexity			
Bc:A:B:Pog			
R	1:−0.0±0.2:0.1±0.4:0.1±0.4	1:0.1:1.0:1.0	— : — : ↑ ↑ : ↑ ↑
L	1:−0.0±0.2:0.1±0.4:0.1±0.4	1:0.1:0.9:0.9	— : — : ↑ ↑ : ↑ ↑

Deviation indicates differences between measurements and mean values. Number of arrows mean deviation range. For example, ↓ ↓ means measurement was smaller than mean within 2 SD.
Diff, differential ratio between left and right values; *Abs,* absolute value of chin prominence; *Rel,* relative ratio of chin prominence.

within this range. The midface angle represents the convexity of the midfacial area. Horizontal and vertical positions of the maxilla and the mandible, as well as their rotation, were observed, and the 3D coordinates of the landmarks and the degree of deviation were recorded. The right and left measurements of the bilateral measurements were recorded simultaneously to observe any differences.

There are some limitations when using 3D CT as a diagnostic tool. We saw relatively large errors in the vertical position (z-coordinate) compared with the anteroposterior (y-coordinate) and transverse (x-coordinate) positions. However, these errors can be decreased if thin slices are used during the reconstruction. The high cost and radiation dose of conventional CT are the major disadvantages, and these can be improved by using cone-beam (CB) CT. The dose of CB CT can be as low as 40 to 50μSv, which is similar to the range of a conventional dental radiographic examination.[18] In addition, in some craniofacial deformities, Or or Po are deviated. Therefore, points in the horizontal plane should not be used as the reference plane. This limitation can also be overcome by CB CT. This is because CB CT can take an image in the natural head position, and the horizontal reference plane can be parallel to the floor, which is not influenced by Or and Po.

Orthodontic diagnosis and treatment planning emphasize the adaptation and proportion of soft tissues.[18,19] In this study, we performed only skeletal analysis. However, many studies have attempted to reproduce the skeleton with dentition and soft-tissue data collected from CT or laser scanners.[6,20,21] A comprehensive analysis including the skeleton, teeth, and soft tissue will be carried out in future studies.

In this study, we proposed the use of 19 measurements that are similar to those used in 2D images.[22] Much information can be obtained with 3D CT, including 3D linear and angular measuring, airway changes, volumetric changes, and muscle changes.[23] Good treatment results can be obtained with a more precise

diagnosis, and the continuous development of 3D analysis will provide more accurate data on a patient.

CONCLUSIONS

Valuable information can be obtained from a 3D CT reconstruction. We proposed a new cephalometric analysis methodology with 3D CT.

REFERENCES

1. Broadbent BH Sr, Broadbent BH Jr, Golden WH. Bolton standards of dentofacial developmental growth. St Louis: Mosby;1975.
2. Baumrind S, Moffitt FH, Curry S. The geometry of three-dimensional measurement from paired coplanar x-ray images. Am J Orthod 1983;84:313-22.
3. Grayson BH, McCarthy JG, Bookstein F. Analysis of craniofacial asymmetry by multiplane cephalometry. Am J Orthod 1983;84:217-24.
4. Grayson BH, LaBatto FA, Kolber AB, McCarthy JG. Basilar multiplane cephalometric analysis. Am J Orthod 1985;88:503-16.
5. Trocme MC, Sather AH, An KN. A biplanar cephalometric stereoradiography technique. Am J Orthod Dentofacial Orthop 1990;98:168-75.
6. Cavalcanti MG, Vannier MW. Quantitative analysis of spiral computed tomography for craniofacial clinical applications. Dentomaxillofac Radiol 1998;27:344-50.
7. Kawamata A, Ariji Y, Langlais RP. Three-dimensional computed tomography imaging in dentistry. Dent Clin North Am 2000;44:395-410.
8. Zemann W, Santler G, Karcher H. Analysis of midface asymmetry in patients with cleft lip, alveolus and palate at the age of 3 months using 3D-COSMOS measuring system. J Craniomaxillofac Surg 2002;30:148-52.
9. Captier G, Leboucq N, Bigorre M, Canovas F, Bonnel F, Bonnafe A, et al. Plagiocephaly: morphometry of skull base asymmetry. Surg Radiol Anat 2003;25:226-33.
10. Quintero JC, Trosien A, Hatcher D, Kapila S. Craniofacial imaging in orthodontics: historical perspective, current status, and future developments. Angle Orthod 1999;69:491-506.
11. Grayson B, Cutting C, Bookstein FL, Kim H, McCarthy JG. The three-dimensional cephalogram: theory, technique, and clinical application. Am J Orthod Dentofacial Orthop 1988;94:327-37.
12. Lee SC. Three-dimensional analysis of facial asymmetry using 2-dimensional cephalometric radiographs [dissertation]. Gwangju, South Korea: Chonnam National University; 2005.
13. Hwang HS, Hwang CH, Lee KH, Kang BC. Maxillofacial 3D image analysis for the diagnosis of facial asymmetry. Am J Orthod Dentofacial Orthop 2006 (in press).
14. Chang HS. A proposal of landmarks for craniofacial analysis using three-dimensional CT imaging [dissertation]. Seoul, South Korea:Yonsei University; 2002.
15. Kim GW. Reproducibility of asymmetry measurements of mandible in three-dimensional CT imaging [dissertation]. Gwangju, South Korea: Chonnam National University;2004.
16. Katusumata A, Fujishita M, Maeda M, Ariji Y, Ariji E, Langlais RO. 3D-CT evaluation of facial asymmetry. Oral Surg Oral Med Oral Pathol Oral Radiol Endod 2005;99:212-20.
17. Bass WM. Human osteology: a laboratory and field manual. 3rd ed. Columbia, Mo: Missouri Archaeological Society; 1987.
18. Graber TM, Vanarsdall RL, Vig KW. Orthodontics: current principles and technique. 4th ed. St. Louis: Mosby; 2005.
19. Baik HS, Jeon JM, Lee HJ. Facial soft tissue analysis of Korean adults with normal occlusion using a 3-dimensional laser scanner. Am J Orthod Dentofacial Orthop 2006 (in press).
20. Han SY. The facial soft tissue analysis of the normal occlusion using three-dimensional CT imaging [dissertation]. Seoul, South Korea:Yonsei University; 2003.
21. Papadopoulos MA, Christou PK, Athanasiou AE, Boettcher P, Zeilhofer HF, Sader R, et al. Three-dimensional craniofacial reconstruction imaging. Oral Surg Oral Med Oral Pathol Oral Radiol Oral Endod 2002;93:382-93.
22. Kane AA, Kim YO, Eaton A, Pilgram TK, Marsh JL, Zonneveld F, et al. Quantification of osseous facial dysmorphology in untreated unilateral coronal synostosis. Plast Reconstr Surg 2000;106:251-8.
23. Kawamata A, Fujishita M, Ariji E. 3D CT evaluation of morphologic airway changes after mandibular setback osteotomy for prognathism. Oral Surg Oral Med Oral Pathol Oral Radiol Endod 2000;89:278-87.